

PERSPECTIVE | OCTOBER 22 2024

InGaN quantum dots for micro-LEDs

Lai Wang ; Luming Yu ; Zhenhao Li ; Anda Cheng ; Zhibiao Hao ; Changzheng Sun ; Bing Xiong ; Yanjun Han; Jian Wang ; Hongtao Li; Lin Gan; Yi Luo



APL Photonics 9, 100904 (2024)

<https://doi.org/10.1063/5.0226660>



Articles You May Be Interested In

Suppression of thermal degradation of InGaN/GaN quantum wells in green laser diode structures during the epitaxial growth

Appl. Phys. Lett. (October 2013)

Optically pumped 500 nm InGaN green lasers grown by plasma-assisted molecular beam epitaxy

J. Appl. Phys. (September 2011)

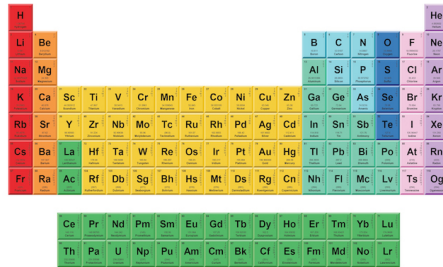
InGaN laser diodes with 50 mW output power emitting at 515 nm

Appl. Phys. Lett. (August 2009)



THE MATERIALS SCIENCE MANUFACTURER®

Now Invent.™



American Elements
Opens a World of Possibilities

...Now Invent!

www.americanelements.com

InGaN quantum dots for micro-LEDs

Cite as: APL Photon. 9, 100904 (2024); doi: [10.1063/5.0226660](https://doi.org/10.1063/5.0226660)

Submitted: 3 July 2024 • Accepted: 4 October 2024 •

Published Online: 22 October 2024



View Online



Export Citation



CrossMark

Lai Wang,^{a)} Luming Yu, Zhenhao Li, Anda Cheng, Zhibiao Hao, Changzheng Sun, Bing Xiong, Yanjun Han, Jian Wang, Hongtao Li, Lin Gan, and Yi Luo

AFFILIATIONS

Beijing National Research Center for Information Science and Technology, Department of Electronic Engineering, Tsinghua University, Beijing 100084, China

^{a)}Author to whom correspondence should be addressed: wanglai@tsinghua.edu.cn

ABSTRACT

Micro-scale light-emitting diodes (micro-LEDs) have received widespread attention in recent years for applications in display and optical communication. Compared with conventional quantum well active regions, quantum dots (QDs) can increase the carrier concentration at the same current density, which is beneficial for improving the efficiency and bandwidth of LEDs at low current densities. This is exactly what micro-LEDs need for display and communication applications. In this Perspective, we give a general introduction to InGaN QDs and provide an overview of the growth of InGaN QDs by metal-organic chemical vapor deposition. We then discuss the advances in green and red micro-LEDs based on InGaN QDs for display applications. This is followed by recent progress on high-speed blue micro-LEDs, which have great potential for use in chip-to-chip optical interconnections. Finally, we address the remaining challenges for a further improvement in InGaN QD-based micro-LEDs.

© 2024 Author(s). All article content, except where otherwise noted, is licensed under a Creative Commons Attribution-NonCommercial-NoDerivs 4.0 International (CC BY-NC-ND) license (<https://creativecommons.org/licenses/by-nc-nd/4.0/>). <https://doi.org/10.1063/5.0226660>

I. INTRODUCTION

In recent years, micro-scale light-emitting diode (micro-LED) has received widespread attention due to its excellent optoelectronic properties, including high brightness, high resolution, high response speed, long lifespan, and low power consumption.^{1–6} The main applications of micro-LEDs are considered to be displays and visible light communication light sources.^{6–8} In the display field, compared with organic light emitting diode (OLED) and LCD, micro-LED has significant brightness advantages and is expected to achieve high-resolution display in outdoor large-screen displays and micro-displays represented by augmented reality (AR) and virtual reality (VR).⁹ In the field of communication, it has been proven that small-sized LED devices can help improve the response speed of chips and break through the device response rate limit.¹⁰ Compared with laser diodes, micro-LEDs as a communication light source offer a lower cost and more relaxed working conditions,^{3–6,11} making them a promising candidate for mainstream communication methods in automotive and home applications. Furthermore, micro-LEDs are expected to achieve the integration of display and communication, aligning with the development trends of future multimedia technology and offering broad development prospects. In addition, micro-LED technology is well-suited for chip-to-chip interconnections,

providing significant advantages such as low bit energy consumption, high bandwidth density, stable high-temperature operation, and low latency, making it particularly beneficial for applications in high-performance computing and artificial intelligence.^{12–16}

However, micro-LEDs also have several problems. First, the efficiency of micro-LED is still low, especially in red ones. Large-sized red LEDs are mainly based on AlGaInP, but more carriers will participate in surface recombination due to higher carrier mobility compared with InGaN LEDs.^{17–19} This is more fatal in micro-LED with a larger specific surface area. In contrast, it is difficult to obtain a high-quality red InGaN active region due to lattice mismatch between GaN and InN.²⁰ In addition, InGaN micro-LEDs will have a blueshift with the increase in current density due to the inherent polarization electric field in the InGaN/GaN quantum well (QW).²¹ As for visible light communication (VLC), the response speed of micro-LED based on polar QW is still insufficient,^{22–27} which is difficult to match with current application requirements and needs further improvement.

InGaN quantum dots (QDs) have become a potential solution to solve these existing issues. QD refers to three-dimensional (3D) particle structures with diameters within 100 nm and similar to the Bohr radius of excitons. Colloidal QDs (usually CdSe–ZnS and other materials) prepared by chemical methods have been applied as color

conversion layers in full-color micro-LED fabrication.²⁸ The concept of semiconductor QDs was first proposed in GaAs materials by Arakawa and Sakaki.²⁹ Compared with two-dimensional QW active regions, QDs exhibit “atomic-like” energy levels rather than energy band structures due to size constraints in all three dimensions. From then on, the buried QD active region has been proven to effectively decrease the threshold and improve the temperature behavior of III-V laser diodes (LDs).^{30,31} Moreover, recent silicon photonics have raised a demand for the heteroepitaxial growth of III-V LDs on silicon substrates, and InAs QD LDs are widely recognized as the best solution to address the issue of high dislocation density.^{32,33} In particular, silicon-based optoelectronic chips often require deep etching of ridge waveguides of LDs for stronger light confinement, and the QDs can alleviate the impact of sidewall etching damage on the active region.^{34,35} This also applies to micro-LEDs as mentioned later.

The study on InGaN QDs started by Narukawa *et al.*³⁶ is driven by their applications in LEDs, LDs, and single photon sources. Banerjee *et al.*³⁷ reported a 550 nm InGaN QD-LD by molecular beam epitaxy (MBE) with a threshold of 0.945 kA/cm², which is significantly lower than that of QW-based LDs. In addition, they have also achieved a 630 nm QD-LD with continuous operation capability.³⁸ Tao *et al.*³⁹ revealed the advantages of using III-nitride QD for high spectral purity and low-chirp laser applications. In addition, the realization of high-quality single photon emission from InGaN QD has been reported.^{40–42}

There have also been reports on the growth of InGaN QDs using MBE. Soto Rodriguez *et al.*⁴³ reported the growth of InGaN QDs on thick InGaN layers with high In composition (>50%) by MBE. Gu *et al.*⁴⁴ reported the self-assembled growth of high-density ($3.0 \times 10^{10} \text{ cm}^{-2}$) and highly uniform InGaN QDs using plasma-assisted molecular beam epitaxy (PA-MBE). Then, they prepared a 20 μm green InGaN QD micro-LED with a peak external quantum efficiency (EQE) of 0.83%.⁴⁵

Some characteristics of InGaN QDs also give them advantages in the fabrication of micro-LEDs. For example, the volume of the QD active region is relatively small, and the same injection current density can achieve a relatively high carrier concentration, which is beneficial for improving efficiency at low current densities; QDs can also alleviate the polarization effect and increase the radiative recombination rate of electrons and holes, which is beneficial for enhancing the bandwidth of micro-LEDs. Because the internal stress of QDs is fully relaxed, the strong piezoelectricity in the traditional InGaN layer will not be generated, so the polarization effect can be suppressed to some extent.

Since metal-organic chemical vapor deposition (MOCVD) is mostly used in industry because of its high efficiency, this Perspective will introduce the epitaxial growth methods of InGaN QDs by MOCVD, which is used for large-scale production of micro-LEDs in industry. Then, the progress of InGaN QDs used to improve the efficiency and bandwidth of micro-LEDs is reported. Finally, the current challenges and future developments of InGaN QD micro-LEDs are summarized.

II. THE EPITAXIAL METHOD OF InGaN QDs

At present, there are two main methods for the epitaxy of InGaN QDs, namely self-assembly growth and selective-area growth

(SAG). SAG QDs should be prepared with a patterned mask in advance, and epitaxy is performed on top to obtain nano-disk or pyramid structures. Wang *et al.* reported a method for preparing InGaN quantum dots using focused ion beam etching technology and selective area growth.⁴⁶ The density and size of QDs grown in this way can be strictly controlled but will inevitably suffer from process damage.⁴⁷ QDs grown on nanowires are expected to solve problems such as lattice mismatch and etching damage.⁴⁸ Pandey *et al.*⁴⁹ demonstrated a new approach to achieve strong red emission (>620 nm) from dislocation-free N-polar InGaN/GaN nanowire-QDs through plasma-assisted MBE. However, so far, there have been no reports of nanowire-QD structures based on MOCVD. MOCVD is less precise than MBE in controlling the growth of nanowire-QDs, especially at the atomic level. In addition, MOCVD is not as effective as MBE in controlling impurities, which is crucial for nanowire-QDs. These may be the potential reasons that may limit the application of MOCVD in nanowire-QDs.

The growth principle of self-assembled QDs is to grow InGaN structures with critical energy/stress, which spontaneously transition from traditional two-dimensional growth to three-dimensional (3D) growth, thus forming the QDs. The epitaxy can be completed in one step, but the morphology, volume, and density of QDs are difficult to control. The most classic QD growth mode is the Stranski-Krastanov (SK) mode, which is characterized by having a QD layer with a bottom 2D substrate layer (also known as a wetting layer). The formation of SK QDs is due to the accumulation of stress in the wetting layer reaching a critical state, which is eventually released through 3D growth. It is worth noting that the generation of QDs and the generation of dislocations are both pathways of stress release, but the former is desirable, while the latter reduces the crystal quality. Zhao *et al.*⁵⁰ pointed out that the critical thickness of 3D growth and dislocation generation are both related to the In component. When the In component is low (typically less than 10%), the critical thickness is extremely large, which will completely mask the morphology of QDs. When the In component is high (typically more than 27%), dislocations will preferentially form, which is not conducive to the formation of QDs. In order to reduce the critical thickness of the wetting layer and reduce its impact on QDs, the growth interruption method can be used to prepare SK QDs. The typical step is to grow an InGaN thin film first, then interrupt the III-V sources, and anneal in a nitrogen atmosphere for a certain time. At this point, atoms migrate on the surface and spontaneously aggregate into QDs.

Multiple results have been reported based on SK QDs with optimized growth conditions. The general schematic diagram of growth steps and the morphology of QDs are shown in Fig. 1(a). The typical density of SK QDs is around 10^8 cm^{-2} .⁵¹ By increasing the growth temperature and switching the carrier gas from N₂ to H₂ during the growth of the GaN barrier, Lv *et al.*⁵² improved the quality and surface morphology of the GaN barrier on QDs, making it possible to grow multi-layer QD active regions. In addition, they also achieved green and red QD-LEDs with low blueshift, and the peak wavelength of the red ones could reach 729 nm.⁵³ By using well-dot coupling structures, Yu *et al.*⁵⁴ demonstrated 520 nm emission QD samples with an internal quantum efficiency (IQE) of up to 21%. Subsequently, Yang *et al.*⁵⁵ optimized the thickness of the tunneling barrier between the well and dot layer and discovered the relationship between QD density and strain. This proves that the essence of

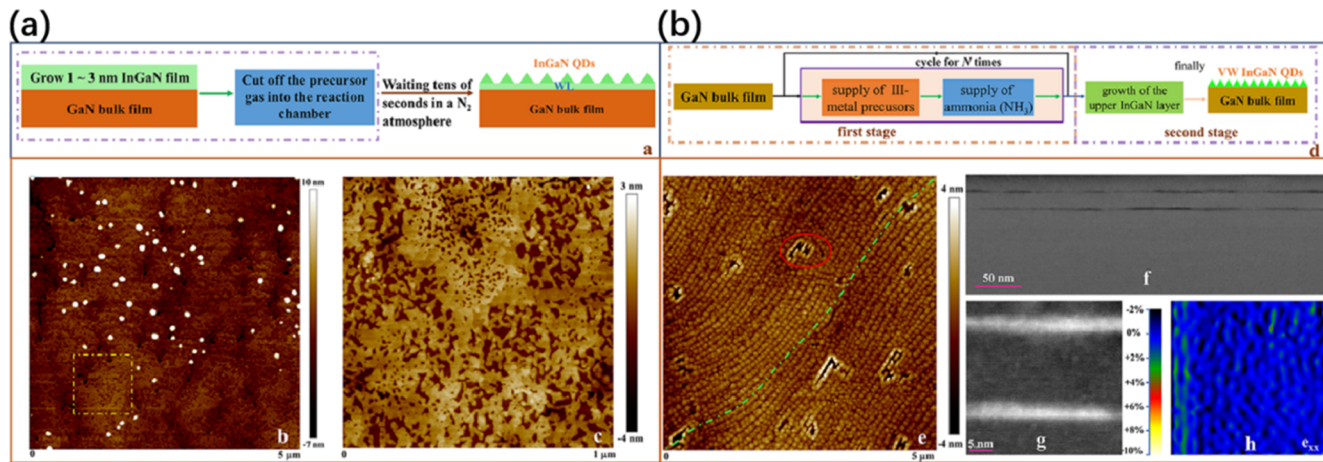


FIG. 1. Typical growth process diagram and morphology of (a) SK mode QDs and (b) VW mode QDs. Reproduced with permission from Wang *et al.*, *Laser Photonics Rev.* 15(5), 2000406 (2021). Copyright 2021 Wiley-VCH GmbH.

the growth interruption method is the decomposition and reassembly of metastable states caused by InGaN phase separation. Based on these results, light-emitting devices using SK QDs have also been proven to have the ability to generate high-quality emissions for the preparation of superluminescent diodes (SLDs) or laser diodes (LDs). Based on a well-dot coupling structure, Wang *et al.*⁵⁶ achieved green SLDs based on QDs, with a wavelength of 526 nm.

Different from SK mode QDs, Volmer–Weber (VW) mode QDs can be grown directly without a wetting layer. Kawasaki *et al.*⁵⁷ have grown VW mode GaN QDs on an AlGaN template by droplet epitaxy. Zhao *et al.*⁵⁸ pointed out that heteroepitaxy conforms to the minimum energy criterion, which means that when other materials are grown on GaN, if the energy of the new system is greater than the surface energy of GaN, the epitaxial layer will directly transition to the 3D growth mode. This theory confirms the feasibility of VW mode InGaN QDs. Recently, VW QDs have also been prepared by MOCVD,⁵¹ using the growth method shown in Fig. 1(b). First, only In and Ga atoms are introduced and adsorbed onto the GaN surface. Since there are no N atoms to react with them, they can freely migrate and eventually aggregate into small 3D nano-island structures. Then, NH₃ is introduced. After thermal decomposition, N atoms reach the substrate surface and react with the metal islands, causing them to be nitrided and nucleated, achieving VW QD morphology. The above process is repeated for a certain number of cycles, that is, periodically alternating the introduction of III/V sources to obtain the QD morphology.⁵⁸ The typical density of VW QDs is around 10^{10} cm^{-2} .⁵¹ The typical emission wavelength of VW QD is $\sim 400 \text{ nm}$, which is difficult to control by changing the growth conditions.

Wang *et al.*⁵¹ reported a wavelength modulation method based on a two-step method, which involves the conformal growth of the InGaN layer on QDs to change the emission wavelength. Through this scheme, the emission wavelength of the device can be controlled over a large range (almost covering visible light range). In the SK mode of growing InGaN QDs, the origin of InGaN QDs stems from the stress caused by the lattice mismatch between InGaN and GaN. Therefore, the prerequisite for stress release to produce QDs is a

sufficient In composition. As a result, the SK mode can only grow QD samples with wavelengths above $\sim 490 \text{ nm}$. A broad spectral coverage is an advantage of the VW mode QDs. In addition, the resulting VW QDs are smaller in size and have improved uniformity.

In addition, an anti-surfactant is also believed to inhibit the wetting layers on the AlGaN surface, which can also promote the formation of QDs.^{59,60} In summary, the growth method of InGaN QDs using the SK mode is relatively simple and does not require a two-step epitaxy. However, the resulting QDs are larger in size, have low density, and have poor uniformity. Moreover, InGaN QDs grown using the VW mode have a broader emission wavelength range. The growth of QDs reflects the precise design of surface energy and reaction kinetics. The morphology of QDs will greatly affect the luminescence performance of the final device. Therefore, optimizing the growth conditions of SK and VW mode QDs will be the core issue of QD-based micro-LED, such as QDs' growth temperature, pressure, alternating on–off source time, flow rate, introducing a pre-strain layer, etc.

III. QD-BASED MICRO-LEDs FOR DISPLAY

According to different usage scenarios, the operating current density range of micro-LEDs needs to have significant differences. Large-screen direct display, represented by high-definition televisions, requires a low operating current density ($\sim 1 \text{ A/cm}^2$), while micro-displays represented by augmented reality (AR) require outdoor operation, requiring extremely high brightness and a high operating current density ($\sim 100 \text{ A/cm}^2$). Due to the fact that the external quantum efficiency (EQE) of LEDs generally has the characteristic of first increasing and then decreasing, it is not realistic to achieve high efficiency within a wide operating range.

In particular, QD-based micro-LEDs have unique advantages in their applications at low current densities. QDs can enhance the carrier confinement effect.^{61–63} Compared to QW-based LEDs, QDs have a higher carrier concentration at the same current density, which helps us suppress non-radiative recombination processes, such as Shockley–Read–Hall (SRH) recombination, that dominate at

low carrier concentrations, resulting in higher efficiency at low operating current densities.⁶⁴ Multiple studies have reported the effect of carrier localization on weakening the size-dependent effects of micro-LED.^{65,66} Due to the strong localization of carriers in QDs, QD-based micro-LEDs are expected to suppress the lateral diffusion of carriers, which weakens the impact of sidewall etching damage on the active region.⁶⁴ For a typical micro-LED chip size ($10\text{--}50\ \mu\text{m}$) and a typical QD density ($10^8\ \text{cm}^{-2}$), there will be about 10^2 QDs in the active region of each micro-LED chip, which means that a small deviation in the number of QDs will hardly affect the emission uniformity of the chip. In addition, due to the sparsity of QDs, only those located exactly on the sidewall will be affected by etching damage, while etching damage in other regions occurs in the GaN barrier layer and will not affect the active region.⁶⁴ This phenomenon is shown in Fig. 2(a). Wang *et al.*⁵¹ confirm the possibility of realizing full-color display with QDs. The EQE of SK QDs for $14\ \mu\text{m}$ green micro-LEDs can reach up to 18%, corresponding to a current density of $0.5\ \text{A}/\text{cm}^2$, which can meet the low working

current density required for panel display applications (applications without high brightness), as shown in Figs. 2(b) and 2(c). The efficiency of VW QDs is relatively low for green devices, but it can still reach 15%. The working current density of VW QDs is higher, which is suitable for outdoor display.

In order to expand the emission wavelength, Yu *et al.*⁸² reported amber micro-LEDs based on VW QDs, with a chip size of $1\text{--}20\ \mu\text{m}$, as shown in Figs. 3(a) -- 3(d). The EQEs of 20 and $1\ \mu\text{m}$ micro-LEDs at 0.3 and $20\ \text{A}/\text{cm}^2$ are 4.92% and 1.78% , respectively. In addition, the peak wavelength is lower than $600\ \text{nm}$ at different injection densities, as shown in Fig. 3(e). Figure 3(f) reveals that by introducing multiple quantum well (MQW) pre-strained layers beneath the QD layers, the luminescence wavelength of the micro-LEDs prepared by sample N is greatly redshifted. A $10\ \mu\text{m}$ micro-LED with $638\ \text{nm}$ emission wavelength is demonstrated, with a price of reduced EQE to 0.03% at $10\ \text{A}/\text{cm}^2$. The results indicate that QDs with longer wavelengths may generate more dislocations; therefore, reducing the number of active region cycles is necessary.

When micro-LEDs need to operate at high current densities, QD micro-LEDs encounter common problems with InGaN materials. As the current density increases, Auger recombination gradually dominates and the luminescence efficiency decreases. In addition, the QD-based micro-LEDs demonstrated in these studies have a relatively large wavelength blueshift, which may be due to the band-filling effect due to the small size of QD. This makes InGaN QDs not suitable for micro-LEDs working under high current densities.

IV. QD-BASED MICRO-LEDs AND COMMUNICATION SYSTEM FOR VISIBLE LIGHT COMMUNICATION (VLC)

Generally speaking, there is a trade-off between luminous efficiency and bandwidth of high-speed LEDs; especially for polar quantum well micro-LEDs, a few kA/cm^2 to tens of kA/cm^2 injection current density is needed to achieve the maximum bandwidth. Because of their smaller structure size and stronger carrier trapping ability, QDs have a higher local carrier concentration and can reach the maximum bandwidth at the order of several hundred A/cm^2 , which is $1\text{--}2$ orders of magnitude lower than that of quantum wells,^{5,14,15,24 -- 27,83 -- 94} as shown in Fig. 4, which is helpful to reduce the bit power consumption in high-speed visible light communication.

Wang *et al.*⁹⁵ utilized the characteristics of phase separation of InGaN materials and the improved growth interruption method to construct the high-speed blue InGaN active region of low-dimensional nanostructure by increasing the temperature, eliminating the upper SK-mode QDs, and strengthening the decomposition, migration, and recombination of metastable and unstable InGaN as shown in Figs. 5(a) -- 5(d). The nanostructure with full stress release increases the spatial overlap integral of the electron–hole wave function and has a higher carrier concentration, so it has a faster carrier recombination rate. Based on single-layer QD-like nanostructures, Wang *et al.*⁹⁵ realized the electrical-to-optical (E–O) bandwidth of $1.3\ \text{GHz}$ through a $75\ \mu\text{m}$ diameter micro-LED. With further scaling down of the chip diameter to $20\ \mu\text{m}$, Li *et al.*¹⁴ achieved the highest bandwidth of InGaN blue micro-LED so far, and experiments verified its operation at $125\ ^\circ\text{C}$, paving the way for chip-to-chip optical interconnection. Its electrical-to-electrical (E–E) $-3\ \text{dB}$ bandwidth of $3.69\ \text{GHz}$ at $1.2\ \text{kA}/\text{cm}^2$ was measured at room temperature and further increased to $3.81\ \text{GHz}$ at $125\ ^\circ\text{C}$ as shown in Figs. 5(f) -- 5(k).

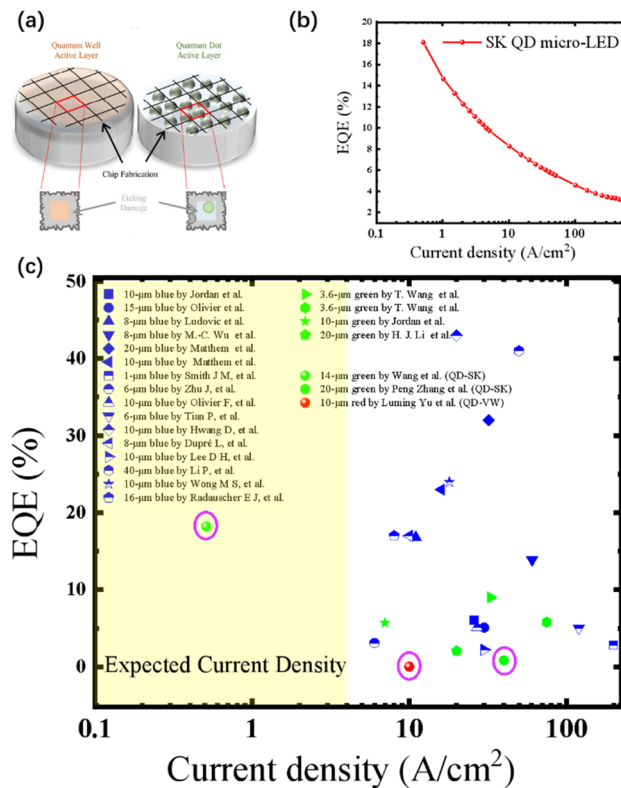


FIG. 2. (a) Schematic of the potential advantages of replacing QWs with QDs as the active region structure. Reproduced with permission from Lu *et al.*, *Laser Photonics Rev.* **16**(12), 2100433 (2022). Copyright 2021 Wiley-VCH GmbH. Electrical properties of SK QD micro-LEDs in the work of Wang *et al.*⁵¹ (b) EQE–current density curves of the QD micro-LED. Reproduced with permission from Wang *et al.*, *Laser Photonics Rev.* **15**(5), 2000406 (2021). Copyright 2021 Wiley-VCH GmbH. (c) Comparison of recently reported results on small-size blue (blue symbols), green (green symbols), and red (red symbols) micro-LEDs (the QD micro-LED labels are circled in purple and all MQDs consist of five periods; the rest are QW micro-LEDs).^{45,51,67,82}

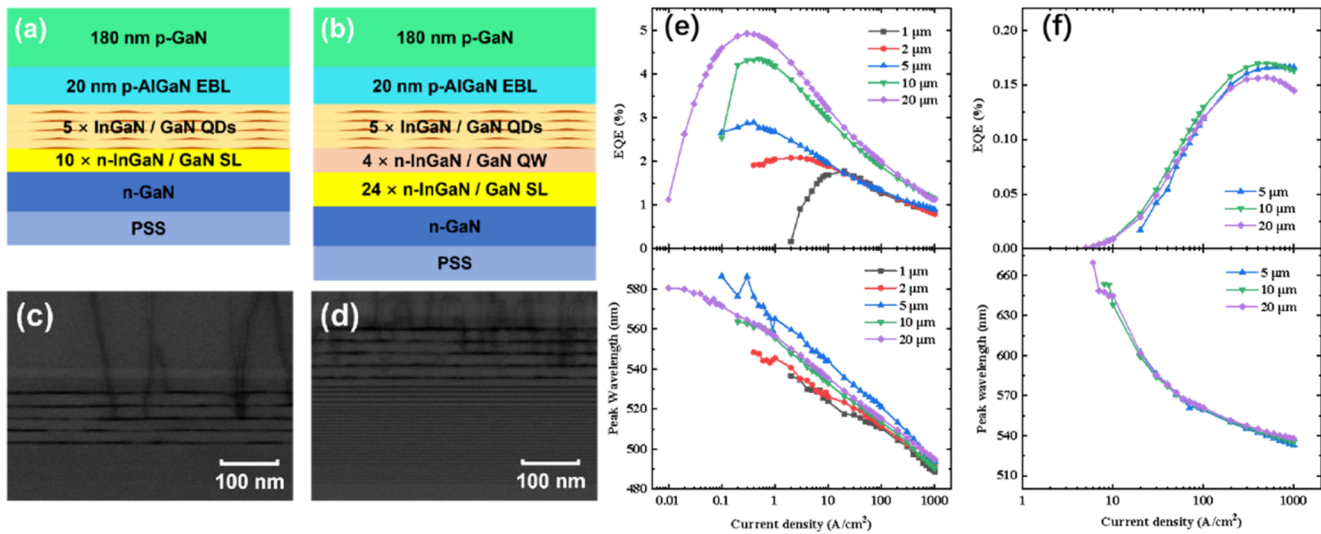


FIG. 3. Red QD micro-LEDs in the work of Yu *et al.*⁸² (a) and (b) Epitaxial structure of sample M and sample N, respectively. (c) and (d) The bright field (BF) STEM image includes superlattice (SL), QD active region, and EBL of sample M and sample N, respectively. The EL characterization of the red InGaN QD micro-LED. (e) EQE (upper) and peak wavelength (lower)-current density diagram of sample M with different sizes. (f) EQE (upper) and peak wavelength (lower)-current density diagram of sample N with different sizes. Reproduced with permission from Yu *et al.*, Opt. Mater. Express 12(8), 3225–3237 (2022). Copyright 2022 Optica Publishing Group.

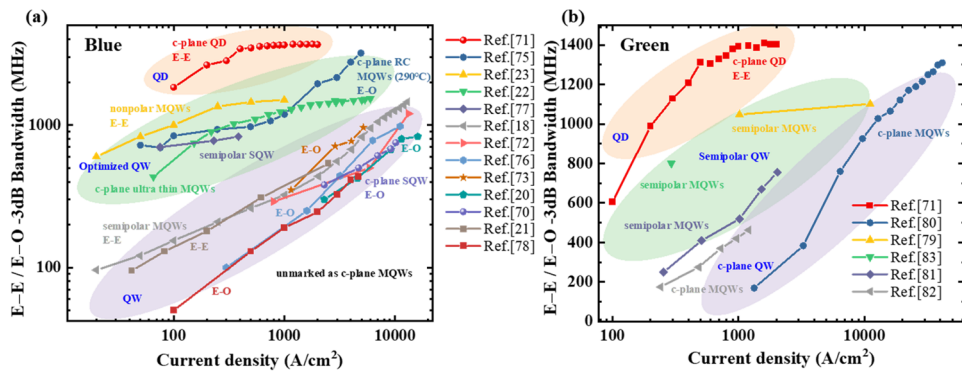


FIG. 4. Relationship between bandwidth and injected current density for (a) blue and (b) green high-speed micro-LEDs in the recent literature. Some studies do not specify whether the bandwidth is measured as E-E or E-O at -3 dB , so this distinction is not indicated in this figure. For clarification, E-O -3 dB bandwidth corresponds to the E-E bandwidth measured at -6 dB .

To characterize the actual communication performance of this kind of micro-LED, Wang *et al.*⁹⁵ and Wei *et al.*⁹⁶ realized the non-return-to-zero (NRZ)-on-off keying (OOK) transmission of 2 Gbps in 3 m free space and 3 m air-underwater link, respectively. Using orthogonal phase shift keying orthogonal frequency division multiplexing (QPSK-OFDM), Wei *et al.*⁹⁷ further enhanced the data rate to 8.75 Gbps. In the 2 m underwater channel, Li *et al.*⁹⁸ used the PAM-4 format to increase the net data rate to 4 Gbps.

Although the aforementioned single-layer quantum dot-like nanostructures have achieved impressive bandwidth, their relatively weak optical power output has limited their effectiveness in practical communication applications. Enhancing the optical power output of these devices while maintaining a high-speed performance is crucial for improving the performance of high-speed micro-LEDs. Li *et al.*¹⁶

addressed this by optimizing the morphology and distribution of the nanostructures using an improved growth interruption method, resulting in a blue micro-LED with a multi-layer nanostructure. When the optical power exceeds 0.5 mW, the -3 dB E-E bandwidth reaches 2.64 GHz. This advancement has enabled a real-time NRZ-OOK communication system that achieves a 0.3 m free-space optical link with a data rate of 3.07 Gbps, a 1 m single-core quartz fiber link with a data rate of 2.60 Gbps, and a 4-channel 0.5 m imaging fiber link with 12.00 Gbps parallel transmission.

Due to the significant increase in the bandwidth of nanostructure micro-LEDs, their limiting factors need to be reexamined. Li *et al.*¹⁴ proposed an equivalent circuit model to analyze these limiting factors. They found that even when the injection current density exceeds $500 \text{ A}/\text{cm}^2$, the bandwidth of a $20 \mu\text{m}$ nanostructure

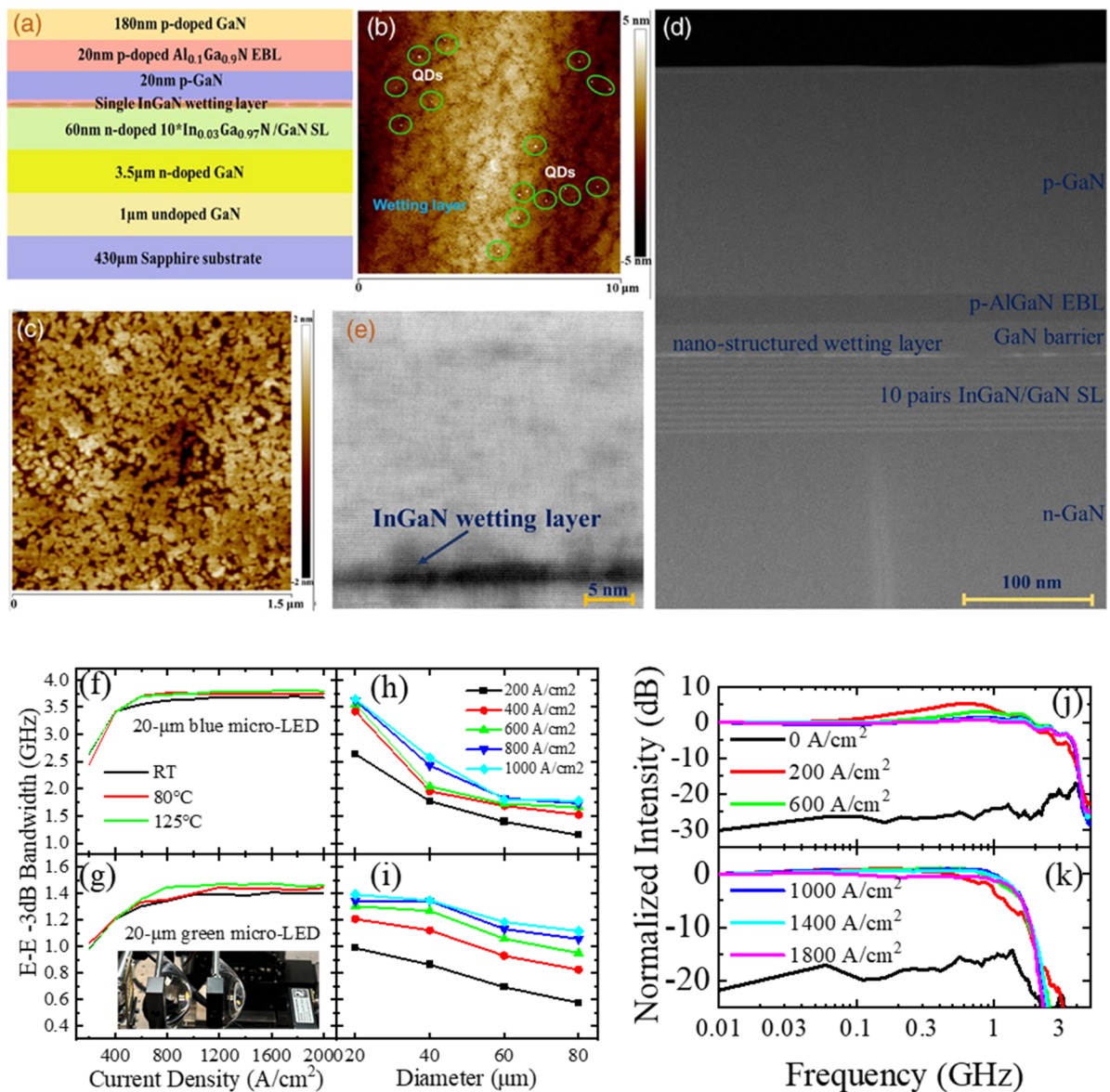


FIG. 5. High-speed blue InGaN low dimensional nanostructure active region in the work of Wang *et al.*⁹⁵ (a) Schematic diagram of the epitaxial structure. The (b) $10 \times 10 \mu\text{m}^2$ and (c) $1.5 \times 1.5 \mu\text{m}^2$ AFM morphology maps. (d) A high-angle annular dark-field (HAADF) STEM image of the LED. (e) A BF STEM image of the nano-structure layer. Reproduced with permission from Wang *et al.*, *Photonics Res.* **9**(5), 792–802 (2021). Copyright 2021 Optica Publishing Group. Bandwidth characteristics of high-speed InGaN blue and green micro-LEDs in the work of Li *et al.*¹⁴ The relationship between the bandwidth and injection current density of 20 μm (f) blue and (g) green micro-LEDs at different temperatures. Inset: the optical link of the bandwidth measurement system. Bandwidth of (h) blue and (i) green micro-LEDs with different diameters. The frequency response of 20 μm (j) blue and (k) green micro-LEDs at room temperature. Reproduced with permission from Li *et al.*, *IEEE Electron Device Lett.* **44**(5), 785–788 (2023). Copyright 2023 Institute of Electrical and Electronics Engineers.

blue micro-LED is still primarily constrained by the RC time constant. Therefore, further miniaturization of the device size would be beneficial for enhancing bandwidth. Li *et al.*⁹⁹ analyzed the effects of device size variation on the non-radiative recombination rate by controlling for the same chip area and comparing single mesa and parallel array micro-LEDs with different sidewall perimeters.

Their analysis revealed that SRH non-radiative recombination does not significantly impact the bandwidth when the injection current density is above $10 \text{ A}/\text{cm}^2$.

Like blue light, green light is also a transparent window in plastic optical fiber and seawater. In order to expand the transmission capacity of the wavelength division multiplexing system, high-speed

green micro-LED is also one of the research hotspots in visible light communication.¹⁰⁰ However, due to the limitation of the green gap, it is difficult to directly increase the indium composition of nanostructures to achieve a high-speed green micro-LED. Taking advantage of the large lattice mismatch between In, Ga metals, and GaN, Wang *et al.*⁵¹ innovatively proposed the alternating on-off source method, which first forms metal droplets and then nitrides them into a quantum dot seed layer without a wetting layer. Based on this seed layer, shape preserving growth of the high In component InGaN has been achieved, achieving high-speed green quantum dots. Based on this, Li *et al.*¹⁴ achieved an E-E -3 dB bandwidth of 1.41 GHz under 1.6 kA/cm² at room temperature, the peak wavelength is about 520 nm, and the bandwidth of 1.48 GHz is obtained at 125 °C. Using the same green QD micro-LED, Wei *et al.*¹⁰¹ demonstrated real-time 2.1 Gbps NRZ-OOK and offline 5 Gbps PAM-4 VLC systems in 2 m free space.

V. SUMMARY AND OUTLOOK

In this Perspective, we give a general introduction to InGaN QDs and provide an overview of the growth of InGaN QDs by MOCVD. QDs grown under SK and VW modes exhibit unique luminescent properties, including high luminescence efficiency and high modulation rate. In addition, QDs may also achieve red-green-blue (RGB) full-color display using GaN-based materials. However, the following are still some issues that need improvement:

- (A) Compared to traditional QW devices, the efficiency of QD-based micro-LEDs is still low. Although the crystal quality inside QDs is good, the growth of QDs still cannot completely avoid the generation of defects in other positions, resulting in insufficient luminescence efficiency. Optimizing the growth conditions of SK and VW mode QDs, such as QDs' growth temperature, pressure, alternating on-off source time, flow rate, and introducing a pre-strain layer, is necessary.
- (B) The FWHM of QD devices is wider, which is related to the uniformity of self-assembled QDs. Although wide FWHM is currently a common issue faced by GaN based materials, improving the airflow control ability in epitaxy to enhance the uniformity of QDs is expected to solve this problem.
- (C) Perfecting the physical model of QD micro-LED devices can help us quantitatively calculate the confinement ability of QDs and design micro-LED devices with higher modulation rates.

ACKNOWLEDGMENTS

All the authors acknowledge the National Key Research and Development Program (Grant No. 2021YFA0716400), the National Natural Science Foundation of China (Grant Nos. 62225405, 62350002, and 61991443), the Key R&D Program of Jiangsu Province, China (Grant No. BE2020004), and the Collaborative Innovation Center of Solid-State Lighting and Energy-Saving Electronics.

AUTHOR DECLARATIONS

Conflict of Interest

The authors have no conflicts to disclose.

Author Contributions

Lai Wang: Writing – review & editing (lead). **Luming Yu:** Writing – original draft (equal). **Zhenhao Li:** Writing – original draft (equal). **Anda Cheng:** Writing – original draft (equal). **Zhibiao Hao:** Supervision (equal). **Changzheng Sun:** Supervision (equal). **Bing Xiong:** Supervision (equal). **Yanjun Han:** Supervision (equal). **Jian Wang:** Supervision (equal). **Hongtao Li:** Supervision (equal). **Lin Gan:** Supervision (equal). **Yi Luo:** Supervision (equal).

DATA AVAILABILITY

Data sharing is not applicable to this article as no new data were created or analyzed in this study.

REFERENCES

- ¹Z. Liu, W. C. Chong, K. M. Wong, and K. M. Lau, "GaN-based LED micro-displays for wearable applications," *Microelectron. Eng.* **148**, 98–103 (2015).
- ²J. Wierer, Jr. and N. Tansu, "III-nitride micro-LEDs for efficient emissive displays," *Laser Photonics Rev.* **13**(9), 1900141 (2019).
- ³D. A. B. Miller, "Attojoule optoelectronics for low-energy information processing and communications," *J. Lightwave Technol.* **35**(3), 346–396 (2017).
- ⁴B. Pezeshki, A. Tselikov, R. Kalman, and E. Afifi, "Parallel microLED-based optical links with record data rates and low power consumption," in *CLEO: Applications and Technology*, 2023.
- ⁵B. Pezeshki, A. Tselikov, R. Kalman, and C. Danesh, "Wide and parallel LED-based optical links using multi-core fiber for chip-to-chip communications," in *Optical Fiber Communication Conference (OFC). OSA Technical Digest* (Optica Publishing Group, 2021), p. F3A.1.
- ⁶K. James Singh, Y. M. Huang, T. Ahmed, A. C. Liu, S. W. Huang Chen, F. J. Liou, T. Z. Wu, C. C. Lin, C. W. Chow, G. R. Lin, and H. C. Kuo, "Micro-LED as a promising candidate for high-speed visible light communication," *Appl. Sci.* **10**(20), 7384 (2020).
- ⁷P. J. Parbrook, B. Corbett, J. Han, T.-Y. Seong, and H. Amano, "Micro-light emitting diode: From chips to applications," *Laser Photonics Rev.* **15**(5), 2000133 (2021).
- ⁸A. D. Griffiths, J. Herrnsdorf, J. J. D. McKendry, M. J. Strain, and M. D. Dawson, "Gallium nitride micro-light-emitting diode structured light sources for multi-modal optical wireless communications systems," *Philos. Trans. R. Soc., A* **378**(2169), 20190185 (2020).
- ⁹Z. Liu, C.-H. Lin, B.-R. Hyun, C.-W. Sher, Z. Lv, B. Luo, F. Jiang, T. Wu, C.-H. Ho, H.-C. Kuo, and J.-H. He, "Micro-light-emitting diodes with quantum dots in display technology," *Light: Sci. Appl.* **9**, 83 (2020).
- ¹⁰L. Yu, L. Wang, Z. Hao, Y. Luo, C. Sun, B. Xiong, Y. Han, J. Wang, and H. Li, "High-speed micro-LEDs for visible light communication: Challenges and progresses," *Semicond. Sci. Technol.* **37**(2), 023001 (2022).
- ¹¹X. W. Xue, F. L. Yan, K. Prifti, F. Wang, B. T. Pan, X. T. Guo, S. J. Zhang, and N. Calabretta, "ROTOPS: A reconfigurable and cost-effective architecture for high-performance optical data center networks," *J. Lightwave Technol.* **38**(13), 3485–3494 (2020).
- ¹²B. Pezeshki, A. Tselikov, R. Kalman, and E. Afifi, "Parallel microLED-based optical links with record data rates and low power consumption," in *CLEO: Applications and Technology 2023* (Optica Publishing Group, 2023), pp. 1–4.

- ¹³B. Pezeshki, A. Tselikov, R. Kalman, and C. Danesh, "Wide and parallel LED-based optical links using multi-core fiber for chip-to-chip communications," in Optical Fiber Communications Conference and Exhibition (OFC), 2021.
- ¹⁴Z. H. Li, X. R. Zhang, Z. B. Hao, Y. Luo, C. Z. Sun, B. Xiong, Y. J. Han, J. Wang, H. T. Li, L. Gan, and L. Wang, "Bandwidth analysis of high-speed InGaN micro-LEDs by an equivalent circuit model," *IEEE Electron Device Lett.* **44**(5), 785–788 (2023).
- ¹⁵B. Pezeshki, R. Kalman, A. Tselikov, and C. Danesh, "High speed light microLEDs for visible wavelength communication," *Proc. SPIE* **11706**, 117060N (2021).
- ¹⁶Z. Li, L. Yu, B. Liu, X. Zhang, Z. Xu, X. Lin, Z. Hao, Y. Luo, C. Sun, B. Xiong, Y. Han, J. Wang, H. Li, L. Gan, N. Chi, and L. Wang, "High-speed micro-LEDs based on nano-engineered InGaN active region towards chip-to-chip interconnections," *J. Lightwave Technol.* **2024**, 1–20 (2024).
- ¹⁷J.-T. Oh, S.-Y. Lee, Y.-T. Moon, J. H. Moon, S. Park, K. Y. Hong, K. Y. Song, C.-H. Oh, J.-I. Shim, H.-H. Jeong, J.-O. Song, H. Amano, and T.-Y. Seong, "Light output performance of red AlGaInP-based light emitting diodes with different chip geometries and structures," *Opt. Express* **26**(9), 11194–11200 (2018).
- ¹⁸M. S. Wong, J. A. Kearns, C. Lee, J. M. Smith, C. Lynsky, G. Lheureux, H. Choi, J. Kim, C. Kim, S. Nakamura, J. S. Speck, and S. P. DenBaars, "Improved performance of AlGaInP red micro-light-emitting diodes with sidewall treatments," *Opt. Express* **28**(4), 5787–5793 (2020).
- ¹⁹Y.-Y. Li, F.-Z. Lin, K.-L. Chi, S.-Y. Weng, G.-Y. Lee, H.-C. Kuo, and C.-C. Lin, "Analysis of size-dependent quantum efficiency in AlGaInP micro-light-emitting diodes with consideration for current leakage," *IEEE Photonics J.* **14**(1), 7007907 (2022).
- ²⁰S. Y. Karpov, "Effect of carrier localization on recombination processes and efficiency of InGaN-based LEDs operating in the 'green gap,'" *Appl. Sci.* **8**(5), 818 (2018).
- ²¹J.-I. Hwang, R. Hashimoto, S. Saito, and S. Nunoue, "Development of InGaN-based red LED grown on (0001) polar surface," *Appl. Phys. Express* **7**(7), 071003 (2014).
- ²²M. Monavarian, A. Rashidi, A. A. Aragon, S. H. Oh, A. K. Rishinaramangalam, S. P. DenBaars, and D. Feezell, "Impact of crystal orientation on the modulation bandwidth of InGaN/GaN light-emitting diodes," *Appl. Phys. Lett.* **112**(4), 041104 (2018).
- ²³Z. Y. Fan, J. Y. Lin, and H. X. Jiang, "III-nitride micro-emitter arrays: Development and applications," *J. Phys. D: Appl. Phys.* **41**(9), 094001 (2008).
- ²⁴R. X. G. Ferreira, E. Xie, J. J. D. McKendry, S. Rajbhandari, H. Chun, G. Faulkner, S. Watson, A. E. Kelly, E. Gu, R. V. Penty, I. H. White, D. C. O'Brien, and M. D. Dawson, "High bandwidth GaN-based micro-LEDs for multi-Gb/s visible light communications," *IEEE Photonics Technol. Lett.* **28**(19), 2023–2026 (2016).
- ²⁵K. Rajabi, J. Wang, J. Jin, Y. Xing, L. Wang, Y. Han, C. Sun, Z. Hao, Y. Luo, K. Qian, C.-J. Chen, and M.-C. Wu, "Improving modulation bandwidth of c-plane GaN-based light-emitting diodes by an ultra-thin quantum wells design," *Opt. Express* **26**(19), 24985–24991 (2018).
- ²⁶F. Xu, Z. Jin, T. Tao, P. Tian, G. Wang, X. Liu, T. Zhi, Q.-a. Yan, D. Pan, Z. Xie, K. Xu, B. Liu, and R. Zhang, "C-plane blue micro-LED with 1.53 GHz bandwidth for high-speed visible light communication," *IEEE Electron Device Lett.* **43**(6), 910–913 (2022).
- ²⁷A. Rashidi, M. Monavarian, A. Aragon, A. Rishinaramangalam, and D. Feezell, "Nonpolar *m*-plane InGaN/GaN micro-scale light-emitting diode with 1.5 GHz modulation bandwidth," *IEEE Electron Device Lett.* **39**(4), 520–523 (2018).
- ²⁸T.-H. Kim, S. Jun, K.-S. Cho, B. L. Choi, and E. Jang, "Bright and stable quantum dots and their applications in full-color displays," *MRS Bull.* **38**(9), 712–720 (2013).
- ²⁹Y. Arakawa and H. Sakaki, "Multidimensional quantum well laser and temperature dependence of its threshold current," *Appl. Phys. Lett.* **40**(11), 939–941 (1982).
- ³⁰T. J. Badcock, R. J. Royce, D. J. Mowbray, M. S. Skolnick, H. Y. Liu, M. Hopkinson, K. M. Groom, and Q. Jiang, "Low threshold current density and negative characteristic temperature 1.3 μm InAs self-assembled quantum dot lasers," *Appl. Phys. Lett.* **90**(11), 111102 (2007).
- ³¹A. Patanè, A. Polimeni, M. Henini, L. Eaves, P. C. Main, and G. Hill, "Thermal effects in quantum dot lasers," *J. Appl. Phys.* **85**(1), 625–627 (1999).
- ³²S. Chen, W. Li, J. Wu, Q. Jiang, M. Tang, S. Shutts, S. N. Elliott, A. Sobiesierski, A. J. Seeds, I. Ross, P. M. Smouton, and H. Liu, "Electrically pumped continuous-wave III-V quantum dot lasers on silicon," *Nat. Photonics* **10**(5), 307 (2016).
- ³³A. Y. Liu, C. Zhang, J. Norman, A. Snyder, D. Lubyshev, J. M. Fastenau, A. W. K. Liu, A. C. Gossard, and J. E. Bowers, "High performance continuous wave 1.3 μm quantum dot lasers on silicon," *Appl. Phys. Lett.* **104**(4), 041104 (2014).
- ³⁴J. C. Norman, Z. Y. Zhang, D. W. Jung, Y. T. Wan, M. J. Kennedy, A. Torres, R. W. Herrick, A. C. Gossard, and J. E. Bowers, "High performance quantum dot lasers epitaxially integrated on Si," *Proc. SPIE* **10771**, 107710D (2018).
- ³⁵J. C. Norman, D. Jung, Z. Y. Zhang, Y. T. Wan, S. T. Liu, C. Shang, R. W. Herrick, W. W. Chow, A. C. Gossard, and J. E. Bowers, "A review of high-performance quantum dot lasers on silicon," *IEEE J. Quantum Electron.* **55**(2), 2000511 (2019).
- ³⁶Y. Narukawa, Y. Kawakami, M. Funato, S. Fujita, S. Fujita, and S. Nakamura, "Role of self-formed InGaN quantum dots for exciton localization in the purple laser diode emitting at 420 nm," *Appl. Phys. Lett.* **70**(8), 981–983 (1997).
- ³⁷A. Banerjee, T. Frost, S. Jahangir, E. Stark, and P. Bhattacharya, "InGaN/GaN self-organized quantum dot lasers grown by molecular beam epitaxy," *J. Cryst. Growth* **378**, 566–570 (2013).
- ³⁸T. Frost, A. Banerjee, and P. Bhattacharya, "Small-signal modulation and differential gain of red-emitting ($\lambda = 630$ nm) InGaN/GaN quantum dot lasers," *Appl. Phys. Lett.* **103**(21), 211111 (2013).
- ³⁹R. Tao, T. Li, J. Yang, Y. Wang, F. Liu, B. Sheng, Z. Huang, S. Yang, L. Yang, X. Rong, T. Wang, B. Shen, Y. Arakawa, and X. Wang, "Impact of quantum dots on III-nitride lasers: A theoretical calculation on linewidth enhancement factors," *IEEE J. Sel. Top. Quantum Electron.* **28**(1: Semiconductor Lasers), 1500107 (2022).
- ⁴⁰M. J. Holmes, T. Zhu, F. C. P. Massabuau, J. Jarman, R. A. Oliver, and Y. Arakawa, "Pure single-photon emission from an InGaN/GaN quantum dot," *APL Mater.* **9**(6), 061106 (2021).
- ⁴¹X. Sun, P. Wang, T. Wang, L. Chen, Z. Chen, K. Gao, T. Aoki, M. Li, J. Zhang, T. Schulz, M. Albrecht, W. Ge, Y. Arakawa, B. Shen, M. Holmes, and X. Wang, "Single-photon emission from isolated monolayer islands of InGaN," *Light: Sci. Appl.* **9**, 159 (2020).
- ⁴²X. Sun, P. Wang, T. Wang, D. Li, Z. Chen, L. Chen, K. Gao, M. Li, J. Zhang, W. Ge, Y. Arakawa, B. Shen, M. Holmes, and X. Wang, "Single photon source based on an InGaN quantum dot in a site-controlled optical horn structure," *Appl. Phys. Lett.* **115**(2), 022101 (2019).
- ⁴³P. E. D. Soto Rodriguez, V. J. Gómez, P. Kumar, E. Calleja, and R. Nötzel, "Near-infrared InN quantum dots on high-In composition InGaN," *Appl. Phys. Lett.* **102**(13), 131909 (2013).
- ⁴⁴Y. Gu, W. X. Yang, P. Zhang, S. Jin, X. F. Li, J. J. Zhu, and S. L. Lu, "Investigation on green micro-LEDs based on self-assembled InGaN quantum dots grown by molecular beam epitaxy," in *IEEE Nanotechnology Materials and Devices Conference (NMDC)* (IEEE, 2022), pp. 6–8.
- ⁴⁵P. Zhang, Y. Gu, Y. Gong, H. W. Hua, S. Jin, W. X. Yang, J. J. Zhu, S. B. Long, and S. L. Lu, "External quantum efficiency enhancement of InGaN-based quantum dot green micro-light-emitting diode arrays by fabricating full-A-sided triangular mesa," *ACS Photonics* **10**(12), 4401–4407 (2023).
- ⁴⁶J. Wang, M. Nozaki, M. Lachab, Y. Ishikawa, R. S. Qhalid Fareed, T. Wang, M. Hao, and S. Sakai, "Metalorganic chemical vapor deposition selective growth and characterization of InGaN quantum dots," *Appl. Phys. Lett.* **75**(7), 950–952 (1999).
- ⁴⁷J. L. Merz, S. Lee, and J. K. Furdyna, "Self-organized growth, ripening, and optical properties of wide-bandgap II-VI quantum dots," *J. Cryst. Growth* **184–185**, 228–236 (1998).
- ⁴⁸C.-C. Lin, Y.-R. Wu, H.-C. Kuo, M. S. Wong, S. P. Denbaars, S. Nakamura, A. Pandey, Z. Mi, P. Tian, K. Ohkawa, D. Iida, T. Wang, Y. Cai, J. Bai, Z. Yang, Y. Qian, S.-T. Wu, J. Han, C. Chen, Z. Liu, B.-R. Hyun, J.-H. Kim, B. Jang, H.-D. Kim, H.-J. Lee, Y.-T. Liu, Y.-H. Lai, Y.-L. Li, W. Meng, H. Shen, B. Liu, X. Wang, K.-l. Liang, C.-J. Luo, and Y.-H. Fang, "The micro-LED roadmap: Status quo and prospects," *J. Phys.: Photonics* **5**(4), 042502 (2023).
- ⁴⁹A. Pandey, J. Min, Y. Malhotra, M. Reddeppa, Y. Xiao, Y. Wu, and Z. Mi, "Strain-engineered N-polar InGaN nanowires: Towards high-efficiency red LEDs on the micrometer scale," *Photonics Res.* **10**(12), 2809–2815 (2022).

- ⁵⁰W. Zhao, L. Wang, J. Wang, Z. Hao, and Y. Luo, "Theoretical study on critical thicknesses of InGaN grown on (0001) GaN," *J. Cryst. Growth* **327**(1), 202–204 (2011).
- ⁵¹L. Wang, L. Wang, C. J. Chen, K. C. Chen, Z. B. Hao, Y. Luo, C. Z. Sun, M. C. Wu, J. D. Yu, Y. J. Han, B. Xiong, J. Wang, and H. T. Li, "Green InGaN quantum dots breaking through efficiency and bandwidth bottlenecks of micro-LEDs," *Laser Photonics Rev.* **15**(5), 2000406 (2021).
- ⁵²W. Lv, L. Wang, J. Wang, Z. Hao, and Y. Luo, "InGaN/GaN multilayer quantum dots yellow-green light-emitting diode with optimized GaN barriers," *Nanoscale Res. Lett.* **7**, 617 (2012).
- ⁵³W. Lv, L. Wang, J. Wang, Y. Xing, J. Zheng, D. Yang, Z. Hao, and Y. Luo, "Green and red light-emitting diodes based on multilayer InGaN/GaN dots grown by growth interruption method," *Jpn. J. Appl. Phys.* **52**(8S), 08JG13 (2013).
- ⁵⁴J. Yu, L. Wang, D. Yang, Z. Hao, Y. Luo, C. Sun, Y. Han, B. Xiong, J. Wang, and H. Li, "Improving the internal quantum efficiency of green InGaN quantum dots through coupled InGaN/GaN quantum well and quantum dot structure," *Appl. Phys. Express* **8**(9), 094001 (2015).
- ⁵⁵D. Yang, L. Wang, Z.-B. Hao, Y. Luo, C. Sun, Y. Han, B. Xiong, J. Wang, and H. Li, "Dislocation analysis of InGaN/GaN quantum dots grown by metal organic chemical vapor deposition," *Superlattices Microstruct.* **99**, 221–225 (2016).
- ⁵⁶L. Wang, L. Wang, J. Yu, Z. Hao, Y. Luo, C. Sun, Y. Han, B. Xiong, J. Wang, and H. Li, "Abnormal Stranski–Krastanov mode growth of green InGaN quantum dots: Morphology, optical properties, and applications in light-emitting devices," *ACS Appl. Mater. Interfaces* **11**(1), 1228–1238 (2019).
- ⁵⁷K. Kawasaki, D. Yamazaki, A. Kinoshita, H. Hirayama, K. Tsutsui, and Y. Aoyagi, "GaN quantum-dot formation by self-assembling droplet epitaxy and application to single-electron transistors," *Appl. Phys. Lett.* **79**(14), 2243–2245 (2001).
- ⁵⁸W. Zhao, L. Wang, J. Wang, W. Lv, Z. Hao, and Y. Luo, "Growth and characterization of self-assembled low-indium composition InGaN nanodots by alternate admittance of precursors," *Phys. Status Solidi A* **209**(6), 1096–1100 (2012).
- ⁵⁹S. Tanaka, S. Iwai, and Y. Aoyagi, "Self-assembling GaN quantum dots on Al_xGa_{1-x}N surfaces using a surfactant," *Appl. Phys. Lett.* **69**(26), 4096–4098 (1996).
- ⁶⁰X. Q. Shen, S. Tanaka, S. Iwai, and Y. Aoyagi, "The formation of GaN dots on Al_xGa_{1-x}N surfaces using Si in GaA-source molecular beam epitaxy," *Appl. Phys. Lett.* **72**(3), 344–346 (1998).
- ⁶¹N. N. Ledentsov, V. M. Ustinov, V. A. Shchukin, P. S. Kop'ev, Z. I. Alferov, and D. Bimberg, "Quantum dot heterostructures: Fabrication, properties, lasers (review)," *Semiconductors* **32**(4), 343–365 (1998).
- ⁶²T. J. Bukowski and J. H. Simmons, "Quantum dot research: Current state and future prospects," *Crit. Rev. Solid State Mater. Sci.* **27**(3–4), 119–142 (2002).
- ⁶³S. Coe-Sullivan, "Quantum dot developments," *Nat. Photonics* **3**(6), 315–316 (2009).
- ⁶⁴B. Y. Lu, L. Wang, Z. B. Hao, Y. Luo, C. J. Chen, M. C. Wu, J. S. Tang, J. K. Kim, and E. F. Schubert, "Dennard scaling in optoelectronics: Scientific challenges and countermeasures of micro-LEDs for displays," *Laser Photonics Rev.* **16**(12), 2100433 (2022).
- ⁶⁵Y. Gu, Y. Gong, P. Zhang, H. W. Hua, S. Jin, W. X. Yang, J. J. Zhu, and S. L. Lu, "Investigation on the optical properties of micro-LEDs based on InGaN quantum dots grown by molecular beam epitaxy," *Nanomaterials* **13**(8), 1346 (2023).
- ⁶⁶X. Zhang, W. X. Yang, Z. W. Xing, H. B. Qiu, Y. Gu, L. F. Bian, S. L. Lu, H. Qin, Y. Cai, Y. Suzuki, S. Kaneko, Y. Matsuda, S. Izumi, Y. Nakamura, and A. Tackeuchi, "Investigation of micromorphology and carrier recombination dynamics for InGaN/GaN multi-quantum dots grown by molecular beam epitaxy," *Crystals* **11**(11), 1312 (2021).
- ⁶⁷J. M. Smith, R. Ley, M. S. Wong, Y. H. Baek, J. H. Kang, C. H. Kim, M. J. Gordon, S. Nakamura, J. S. Speck, and S. P. DenBaars, "Comparison of size-dependent characteristics of blue and green InGaN microLEDs down to 1 μm in diameter," *Appl. Phys. Lett.* **116**(7), 071102 (2020).
- ⁶⁸F. Olivier, S. Tirano, L. Dupre, B. Aventurier, C. Largeron, and F. Templier, "Influence of size-reduction on the performances of GaN-based micro-LEDs for display application," *J. Lumin.* **191**, 112–116 (2017).
- ⁶⁹L. Dupré, M. Marra, V. Verney, B. Aventurier, F. Henry, F. Olivier, S. Tirano, A. Daami, and F. Templier, "Processing and characterization of high resolution GaN/InGaN LED arrays at 10 micron pitch for micro display applications," *Proc. SPIE* **10104**, 1010422 (2017).
- ⁷⁰C.-J. Chen, H.-C. Chen, J.-H. Liao, C.-J. Yu, and M.-C. Wu, "Fabrication and characterization of active-matrix 960 × 540 blue GaN-based micro-LED display," *IEEE J. Quantum Electron.* **55**(2), 3300106 (2019).
- ⁷¹M. S. Wong, D. Hwang, A. I. Alhassan, C. Lee, R. Ley, S. Nakamura, and S. P. DenBaars, "High efficiency of III-nitride micro-light-emitting diodes by sidewall passivation using atomic layer deposition," *Opt. Express* **26**(16), 21324–21331 (2018).
- ⁷²M. S. Wong, C. Lee, D. J. Myers, D. Hwang, J. A. Kearns, T. Li, J. S. Speck, S. Nakamura, and S. P. DenBaars, "Size-independent peak efficiency of III-nitride micro-light-emitting-diodes using chemical treatment and sidewall passivation," *Appl. Phys. Express* **12**(9), 097004 (2019).
- ⁷³H. Li, M. S. Wong, M. Khouri, B. Bonef, H. Zhang, Y. Chow, P. Li, J. Kearns, A. A. Taylor, P. De Mierry, Z. Hassan, S. Nakamura, and S. P. DenBaars, "Study of efficient semipolar (11-22) InGaN green micro-light-emitting diodes on high-quality (11-22) GaN/sapphire template," *Opt. Express* **27**(17), 24154–24160 (2019).
- ⁷⁴J. Bai, Y. Cai, P. Feng, P. Fletcher, C. Zhu, Y. Tian, and T. Wang, "Ultrasmall, ultracompat and ultrahigh efficient InGaN micro light emitting diodes (μLEDs) with narrow spectral line width," *ACS Nano* **14**(6), 6906–6911 (2020).
- ⁷⁵J. Bai, Y. Cai, P. Feng, P. Fletcher, X. Zhao, C. Zhu, and T. Wang, "A direct epitaxial approach to achieving ultrasmall and ultrabright InGaN micro light-emitting diodes (μLEDs)," *ACS Photonics* **7**(2), 411–415 (2020).
- ⁷⁶J. Zhu, T. Takahashi, D. Ohori, K. Endo, S. Samukawa, M. Shimizu, and X. L. Wang, "Near-complete elimination of size-dependent efficiency decrease in GaN micro-light-emitting diodes," *Phys. Status Solidi A* **216**(22), 1970075 (2019).
- ⁷⁷P. F. Tian, J. J. D. McKendry, Z. Gong, B. Guilhabert, I. M. Watson, E. D. Gu, Z. Z. Chen, G. Y. Zhang, and M. D. Dawson, "Size-dependent efficiency and efficiency droop of blue InGaN micro-light emitting diodes," *Appl. Phys. Lett.* **101**(23), 231110 (2012).
- ⁷⁸D. Hwang, A. Mughal, C. D. Pynn, S. Nakamura, and S. P. DenBaars, "Sustained high external quantum efficiency in ultrasmall blue III-nitride micro-LEDs," *Appl. Phys. Express* **10**(3), 032101 (2017).
- ⁷⁹H. Lee, J. H. Lee, J. S. Park, T. Y. Seong, and H. Amano, "Improving the leakage characteristics and efficiency of GaN-based micro-light-emitting diode with optimized passivation," *ECS J. Solid State Sci. Technol.* **9**(5), 055001 (2020).
- ⁸⁰P. P. Li, H. J. Zhang, H. J. Li, M. Iza, Y. F. Yao, M. S. Wong, N. Palmquist, J. S. Speck, S. Nakamura, and S. P. DenBaars, "Size-independent low voltage of InGaN micro-light-emitting diodes with epitaxial tunnel junctions using selective area growth by metalorganic chemical vapor deposition," *Opt. Express* **28**(13), 18707–18712 (2020).
- ⁸¹E. J. Radauscher, M. Meitl, C. Prevatte, S. Bonafede, R. Rotzoll, D. Gomez, T. Moore, B. Raymond, R. Cok, A. Fecioru, A. J. Trindade, B. Fisher, S. Goodwin, P. Hines, G. Melnik, S. Barnhill, and C. A. Bower, "Miniaturized LEDs for flat-panel displays," *Proc. SPIE* **10124**, 1012418 (2017).
- ⁸²L. M. Yu, L. Wang, P. L. Yang, Z. B. Hao, J. D. Yu, Y. Luo, C. Z. Sun, B. Xiong, Y. J. Han, J. Wang, H. T. Li, and L. Wang, "Metal organic vapor phase epitaxy of high-indium-composition InGaN quantum dots towards red micro-LEDs," *Opt. Mater. Express* **12**(8), 3225–3237 (2022).
- ⁸³H. Y. Lan, I. C. Tseng, H. Y. Kao, Y. H. Lin, G. R. Lin, and C. H. Wu, "752-MHz modulation bandwidth of high-speed blue micro light-emitting diodes," *IEEE J. Quantum Electron.* **54**(5), 3300106 (2018).
- ⁸⁴Y. Cai, J. I. H. Haggar, C. Zhu, P. Feng, J. Bai, and T. Wang, "Direct epitaxial approach to achieve a monolithic on-chip integration of a HEMT and a single micro-LED with a high-modulation bandwidth," *ACS Appl. Electron. Mater.* **3**(1), 445–450 (2021).
- ⁸⁵J. Vinogradov, R. Kruglov, R. Engelbrecht, O. Zieman, J. K. Sheu, K. L. Chi, J. M. Wun, and J. W. Shi, "GaN-based cyan light-emitting diode with up to 1-GHz bandwidth for high-speed transmission over SI-POF," *IEEE Photonics J.* **9**(3), 7201707 (2017).

- ⁸⁶D. Rogers, H. Xue, F. Kish, B. Pezeski, A. Tselikov, and J. J. Wierer, "High temperature and large bandwidth blue InGaN/GaN micro-LEDs," in *Optical Fiber Communication Conference (OFC) 2024. Technical Digest Series* (Optica Publishing Group, 2024), p. Th3D.6.
- ⁸⁷E. Xie, R. Bian, X. He, M. S. Islim, C. Chen, J. J. D. McKendry, E. Gu, H. Haas, and M. D. Dawson, "Over 10 Gbps VLC for long-distance applications using a GaN-based series-biased micro-LED array," *IEEE Photonics Technol. Lett.* **32**(9), 499–502 (2020).
- ⁸⁸M. Haemmer, B. Roycroft, M. Akhter, D. V. Dinh, Z. Quan, J. Zhao, P. J. Parbrook, and B. Corbett, "Size-dependent bandwidth of semipolar (1122) light-emitting-diodes," *IEEE Photonics Technol. Lett.* **30**(5), 439–442 (2018).
- ⁸⁹J. J. D. McKendry, D. Massoubre, S. Zhang, B. R. Rae, R. P. Green, E. Gu, R. K. Henderson, A. E. Kelly, and M. D. Dawson, "Visible-light communications using a CMOS-controlled micro-light-emitting-diode array," *J. Lightwave Technol.* **30**(1), 61–67 (2012).
- ⁹⁰Y. H. Chang, Y. M. Huang, W. H. Gunawan, G. H. Chang, F. J. Liou, C. W. Chow, H. C. Kuo, Y. Liu, and C. H. Yeh, "4.343-Gbit/s green semipolar (20–21) μ -LED for high speed visible light communication," *IEEE Photonics J.* **13**(4), 7300204 (2021).
- ⁹¹R. Lin, Z. Jin, P. Qiu, Y. Liao, J. Hoo, S. Guo, X. Cui, and P. Tian, "High bandwidth series-biased green micro-LED array toward 6 Gbps visible light communication," *Opt. Lett.* **47**(13), 3343–3346 (2022).
- ⁹²S.-W. H. Chen, Y.-M. Huang, Y.-H. Chang, Y. Lin, F.-J. Liou, Y.-C. Hsu, J. Song, J. Choi, C.-W. Chow, C.-C. Lin, R.-H. Horng, Z. Chen, J. Han, T. Wu, and H.-C. Kuo, "High-bandwidth green semipolar (20–21) InGaN/GaN micro light-emitting diodes for visible light communication," *ACS Photonics* **7**(8), 2228–2235 (2020).
- ⁹³C. L. Liao, C. L. Ho, Y. F. Chang, C. H. Wu, and M. C. Wu, "High-speed light-emitting diodes emitting at 500 nm with 463-MHz modulation bandwidth," *IEEE Electron Device Lett.* **35**(5), 563–565 (2014).
- ⁹⁴G.-R. Lin, H.-C. Kuo, C.-H. Cheng, Y.-C. Wu, Y.-M. Huang, F.-J. Liou, and Y.-C. Lee, "Ultrafast 2 \times 2 green micro-LED array for optical wireless communication beyond 5 Gbit/s," *Photonics Res.* **9**(10), 2077–2087 (2021).
- ⁹⁵L. Wang, Z. Wei, C.-J. Chen, L. Wang, H. Y. Fu, L. Zhang, K.-C. Chen, M.-C. Wu, Y. Dong, Z. Hao, and Y. Luo, "1.3 GHz E-O bandwidth GaN-based micro-LED for multi-gigabit visible light communication," *Photonics Res.* **9**(5), 792–802 (2021).
- ⁹⁶Z. Wei, L. Zhang, L. Wang, C.-J. Chen, A. Pepe, X. Liu, K.-C. Chen, M.-C. Wu, Y. Dong, L. Wang, Y. Luo, and H. Y. Fu, "2 Gbps/3 m air-underwater optical wireless communication based on a single-layer quantum dot blue micro-LED," *Opt. Lett.* **45**(9), 2616–2619 (2020).
- ⁹⁷Z. Wei, Z. Liu, X. Liu, L. Wang, L. Wang, C. Yu, and H. Y. Fu, "8.75 Gbps visible light communication link using an artificial neural network equalizer and a single-pixel blue micro-LED," *Opt. Lett.* **46**(18), 4670–4673 (2021).
- ⁹⁸X. Li, C. Cheng, C. Zhang, Z. Wei, L. Wang, H. Y. Fu, and Y. Yang, "Net 4 Gb/s underwater optical wireless communication system over 2 m using a single-pixel GaN-based blue mini-LED and linear equalization," *Opt. Lett.* **47**(8), 1976–1979 (2022).
- ⁹⁹Z. Li, X. Zhang, L. Yu, B. Liu, Z. Hao, Y. Luo, C. Sun, B. Xiong, Y. Han, J. Wang, H. Li, L. Gan, and L. Wang, "Research on high-speed micro-LED parallel chips," in *The 2023 Chinese Optical Society Academic Conference*, 2023.
- ¹⁰⁰Z. Wei, L. Wang, Z. Li, C.-J. Chen, M.-C. Wu, L. Wang, and H. Y. Fu, "Micro-LEDs illuminate visible light communication," *IEEE Commun. Mag.* **61**(4), 108–114 (2023).
- ¹⁰¹Z. Wei, L. Wang, Z. Liu, C. Zhang, C.-J. Chen, M.-C. Wu, Y. Yang, C. Yu, L. Wang, and H. Y. Fu, "Multigigabit visible light communication based on high-bandwidth InGaN quantum dot green micro-LED," *ACS Photonics* **9**(7), 2354–2366 (2022).